Structural Innovation: Combining Classic Theories with New Technologies

WILLIAM F. BAKER, LAUREN L. BEGHINI, ARKADIUSZ MAZUREK, JUAN CARRION and ALESSANDRO BEGHINI

ABSTRACT

In the early stages of the design process, an engineer sets the geometry of the structure. The decisions made about the layout of the structure will determine the overall efficiency that can be achieved and the magnitude of the forces that must be accommodated. For example, the deflection of a truss can actually be decreased by removing material if a geometry is created that has a shorter total load path. This paper presents concepts and methodologies for creating and understanding efficient geometries. It starts with a review of the 19th- and 20th-century load path theories of Rankine, Maxwell, Cremona and Michell. It then combines their insights with current topology optimization and shape-finding tools as a means of exploring how engineers can create structural geometries that improve the behavior and reduce the tonnage of their designs. Several examples of classical theoretical solutions are explored along with their application to new designs.

Keywords: structural geometry, structural efficiency, structural analysis.

INTRODUCTION

The success of any project depends on starting with a good concept. For the design of structural steel trusses and other structures, the geometrical arrangement of the members is often the most important consideration in producing an efficient and well-behaved design. Although efficiency has always been a chief design consideration, its importance has increased lately as designers seek to minimize the carbon footprint in the construction of new structures. Where can the designer seek guidance in creating layouts that achieve the goals of efficiency and good behavior? A good place to begin is at the start of modern structural engineering.

The mid-19th century was a key period in the advancement of the understanding of structural behavior. The theory of elasticity had already been highly advanced through the development of elastic "aether" theories, and many mathematicians, scientists and natural philosophers were extending their studies into structural mechanics, as well as optics, electricity and magnetism. Their interest in structures was undoubtedly further influenced by the advent of the railroad.

The emergence of railroads led to technological challenges and advancements. The railroads needed bridges and, as a response, the first metal truss bridge was built in the United States in 1840 and in the United Kingdom in 1845 (Timoshenko, 1953). The great thinkers of the time began focusing their thoughts upon the practical issues of trusses and bridges and, in doing so, pushed the limits of structural engineering. One such example is the British Astronomer Royal, George Biddell Airy, who not only studied the stars, but also developed his famous Airy stress function in response to Stephenson's Britannia Bridge (Airy, 1863).

This paper reviews some important works by Rankine, Maxwell, Cremona and Michell that still have great relevance to modern design. Today's structural engineer can combine the ideas of these great innovators with modern topology optimization tools to develop structural concepts for steel trusses and other structures. By combining these concepts with practical considerations of constructability and cost, the structural engineer can develop responsible designs that can minimize the carbon footprint in the construction of new structures and help reduce the consumption of our natural resources.

Please note the theories and findings included in this paper are based on equilibrium and compatibility and, when calculating volume, strength or deflection, constitutive relationships assuming linearly elastic material. The analysis and exploration of the effects of geometric and material nonlinearites on optimal topology layouts is under investigation by a number of researchers.

William F. Baker, P.E., S.E., Partner, Skidmore, Owings & Merrill LLP, Chicago, IL (corresponding). Email: william.baker@som.com

Lauren L. Beghini, Ph.D., Structural Engineer, Skidmore, Owings & Merrill LLP, Chicago, IL. Email: lauren.beghini@gmail.com

Arkadiusz Mazurek, Ph.D., P.E., S.E., Associate, Skidmore, Owings & Merrill LLP, Chicago, IL. Email: arkadiusz.mazurek@som.com

Juan Carrion, Ph.D., P.E., Structural Consultant, Skidmore, Owings & Merrill LLP, Chicago, IL. Email: juan.carrion@som.com

Alessandro Beghini, Ph.D., P.E., S.E., Associate, Skidmore, Owings & Merrill LLP, San Francisco, CA. Email: alessandro.beghini@som.com

MAXWELL'S THEOREM ON LOAD PATHS

When famously asked if he had stood on the shoulders of Newton, Albert Einstein replied, "That statement is not quite right. I stood on Maxwell's shoulders" (Forfar, 2012). James Clerk Maxwell was one of the greatest thinkers of the 19th century and, although best known for his work in electromagnetic theory, his influence extends to various other scientific subjects, including significant work in structural engineering.

In his 1864 paper, "On Reciprocal Figures and Diagrams of Forces," Maxwell [who begins his paper with a reference to Rankine's (1864) work on the equilibrium of polyhedral trusses] developed a theorem that essentially states that the sum of a structure's tension load paths minus the sum of the compression load paths is equal to a value related to the applied external forces (including reactions). In this paper, the term *load path* for a structure or group of members refers to the sum of the axial force in each member times its length. Expressed as an equation, Maxwell's theorem can be written as follows (Cox, 1965):

$$\sum F_T L_T - \sum F_C L_C = \sum \overline{P_i} \cdot \overline{r_i} \tag{1}$$

The value on the right side is the dot product of all the external forces, $\overline{P_i}$, with position vectors from an arbitrary origin, $\overline{r_i}$. This dot product ($\sum \overline{P_i} \cdot \overline{r_i} = |\overline{P_i}||\overline{r_i}| \cos\theta$, where θ is the angle between vectors $\overline{P_i}$ and $\overline{r_i}$) can be viewed as a representation of the negative of the work it takes for all the external forces to cancel all the reactions. Its proof is straightforward: If there is a truss with a series of applied external loads that are in equilibrium with a set of internal forces (see Figure 1) and, from an arbitrary point, if the space is dilated so that all the nodes become twice as far from the origin as they were originally, all the tension forces will do positive work equal to the tensile force in each member times the member length. The compression members will also double in length but will do negative work. From conservation of energy, the total internal work will be equal to the work done by the external forces, which is equal to the dot product on the right side.
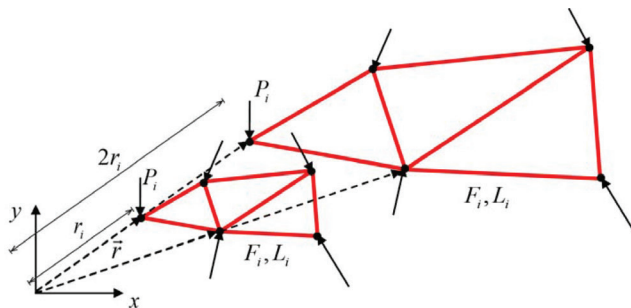
While this theorem has generally been lost to the engineering profession, it represents a very powerful idea that has great potential in the design of trusses. It tells us that the longer the total tension load path, the longer the compression load path must be for a set of external loads of given magnitude, direction and position. Stated another way, if a tension (or compression) load path is "too long," the truss will be penalized twice—once in tension and once in compression. Thus, if we can find a configuration that minimizes the tension load path, the compression load path will automatically be minimized and vice versa.

A further observation is that if a structure only has tension members or only has compression members, it is already a structure of minimal load path, assuming that the points of applied loads and reactions do not change as the geometry of the structure changes.

Figure 2 shows an illustration of Maxwell's theorem using the loads and supports of a cantilever with a 3:1 span. If the origin is placed at the lower left point of the cantilever, the dot product can be easily calculated and is equal to *PB*. Thus, according to Maxwell's theorem, the difference between the tension load path and the compression load path is *PB*.

It can also be shown that the constant *PB* represents the negative of the work needed for the applied loads and reactions to cancel each other. For example, by moving the two horizontal forces together to cancel one another, zero work is done because the movement is perpendicular to the direction of the forces. Furthermore, if the vertical force at the lower right of the cantilever were to be moved and placed directly below the upper vertical load, zero work is still done but, as this load is moved to the point in which the vertical loads are canceled, negative work equal to Maxwell's constant *PB* is done.

LOAD PATHS OF DIFFERENT TRUSS GEOMETRIES

The efficiency of the cantilever constructed to carry the loads shown in Figure 2 can be examined by considering a series of different truss geometries. For example, the first considered geometry might be the moment diagram, which, although it has the shortest path, is not the shortest
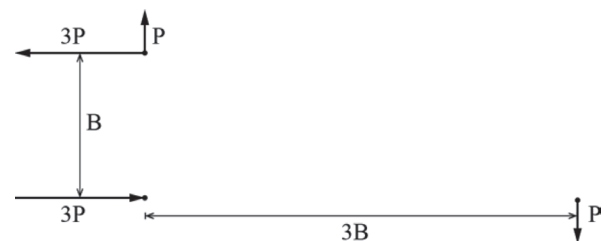

Fig. 1. Geometrical proof of Maxwell's theorem.

Fig. 2. Illustration of Maxwell's theorem using a 3:1 cantilever.

load path structure (Figure 3). Here, the force in the tension member times its length gives the total tensile load path $\sum F_T L_T = 10PB$, while the force in the compression member times its length results in a total compressive load path of $\sum F_C L_C = 9PB$, resulting in a difference of $\sum F_T L_T - \sum F_C L_C = PB$, as predicted by Maxwell's theorem. The total load path is $\sum F_T L_T + \sum F_C L_C = 19PB$. But how much would such a truss deflect? Using the Principle of Virtual Work, the deflection can be expressed as follows:

$$\Delta = \sum \frac{nFL}{EA} \qquad (2)$$

and, if this is a fully stressed structure with equal stresses in tension and compression, the truss will deflect by $19\sigma B/E$.

Another classic solution to the 3:1 cantilever is the Pratt truss (Figure 4). Here, the summation of the tension member forces times their corresponding lengths is $\sum F_T L_T = 9PB$, and the summation of the compression member forces times their corresponding lengths is $\sum F_C L_C = 8PB$. The difference is once again Maxwell's constant, PB, but the total load path has decreased to $17PB$, while the deflection has decreased to $17\sigma B/E$. Although the Pratt truss has a higher total length of members, it has a shorter load path; the change in geometry decreases the total load path and, correspondingly, the deflection.

A closer examination of the Pratt truss reveals that the diagonals carry the loads from the point of load application to the reactions at the supports. The verticals do not carry the loads closer to the supports of the truss; can they, then, be replaced with a different layout? This observation prompts an examination of a Warren truss (Figure 5). In this type of truss, the tension load path is further reduced to $\sum F_T L_T = 8PB$, and the compression load path is reduced to $\sum F_C L_C = 7PB$. While the difference remains at PB, the total load path has been further reduced to $15PB$, and the corresponding deflection is reduced to $15\sigma B/E$. By changing the geometry of the structure, it is possible to reduce the volume of material and make it stiffer—a remarkable achievement.

Figure 6 shows a truss with a still shorter load path. It represents a minimum load path solution for a structure with a geometry bounded to a depth B and 12 members. Although it appears a bit unusual, the geometry is very regular with the intersection of all the tension and compression members happening at nearly the same angle. If the angles are made to be the same, the load path only increases 0.03%. For a span to depth ratio of 2.63:1, the angle between the tension and compression members will be 60 degrees, and the triangles become 30/60/90 right triangles. The solution in Figure 6 provides a benchmark for judging the efficiency of other geometries.

Minimum load path is not the only consideration in selecting a final solution. For example, the designer needs to consider issues such as complexity, cost, usability, aesthetics, multiple loading conditions and permitted stresses
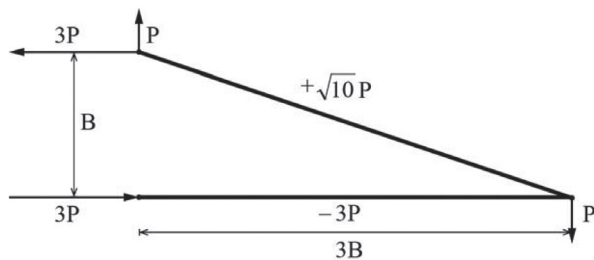

Fig. 3. Truss geometry selected for shortest path,
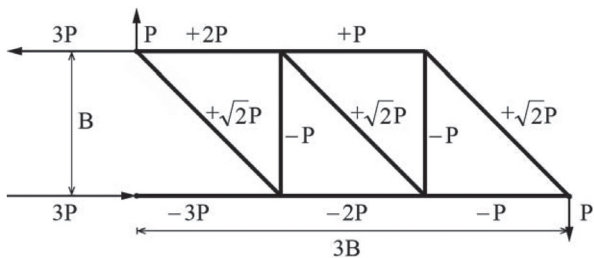which coincides with the moment diagram.
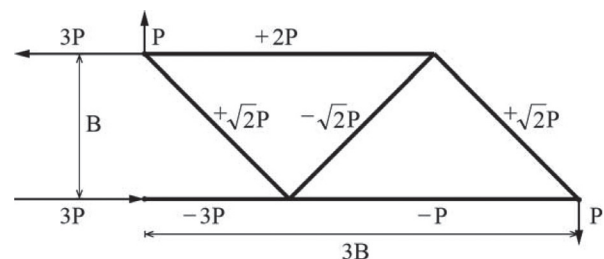

Fig. 5. Geometry of a Warren truss.

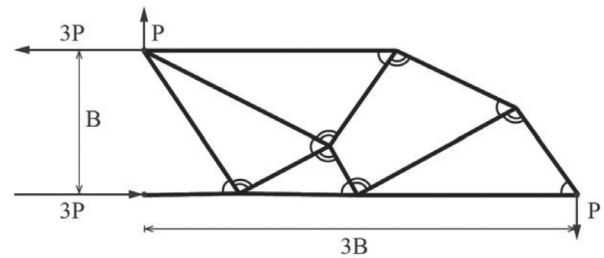Fig. 4. Geometry of a Pratt truss.

Fig. 6. Bounded optimal truss with 12 members.

Table 1. Load Path and Deflection Comparisons for 3:1 Cantilever					
	Tensile Load Path, $\sum F_T L_T$	Compressive Load Path, $\sum F_C L_C$	Difference in Load Paths, $\sum F_T L_T - \sum F_C L_C$	Sum of Load Paths, $\sum F_T L_T + \sum F_C L_C$	Deflection, Δ
Moment diagram truss	10PB	9PB	PB	19PB	$19\dfrac{\sigma B}{E}$
Pratt truss	9PB	8PB	PB	17PB	$17\dfrac{\sigma B}{E}$
Warren truss	8PB	7PB	PB	15PB	$15\dfrac{\sigma B}{E}$
Bounded optimal truss	7.7PB	6.7PB	PB	14.47PB	$14.47\dfrac{\sigma B}{E}$
Compression chord cantilever	8.52PB	7.52PB	PB	16.04PB	$16.04\dfrac{\sigma B}{E}$

for tension and compression. For example, if the designer decides to limit the number of compression members to a minimum, Figure 7 provides a solution. Once again, this structure is very regular, with all the tension members from the support intersecting the compression chord at the same angle. A comparison to the geometry in Figure 6 shows that the Figure 7 geometry has a load path that is 10.9% larger.

A comparison of these geometries is provided in Table 1. It is advised that the reader study the relationships among the internal forces, total load paths and deflections to develop his or her own insight into the problem.

Deflections are often an important consideration in the design of structures. If a structure is uniformly stressed, the relative volume of steel needed by alternate truss geometries to achieve a target deflection can be shown equal to the square of the ratio of the load paths. This can be shown as follows.

If the volumes of any two structures in Table 1 are compared with one another, we have:

Fig. 7. Cantilever with only compression chord.

$$V_1 = \frac{\alpha_1 PB}{\sigma_1} \tag{3}$$

and

$$V_2 = \frac{\alpha_2 PB}{\sigma_2} \tag{4}$$

where α represents the coefficient of the sum of the load paths in Table 1. Because the deflection is set to be equal,

$$\Delta = \alpha_1 \sigma_1 \frac{B}{E} = \alpha_2 \sigma_2 \frac{B}{E} \Rightarrow \sigma_2 = \frac{\alpha_1}{\alpha_2} \sigma_1 \tag{5}$$

Thus, the ratio of the volumes can be computed as

$$\frac{V_2}{V_1} = \frac{\dfrac{\alpha_2^2 PB}{\alpha_1 \sigma_1}}{\dfrac{\alpha_1 PB}{\sigma_1}} = \left(\frac{\alpha_2}{\alpha_1}\right)^2 \tag{6}$$

This example shows that load path is a major consideration in the efficiency of deflection-controlled designs. For example, the Pratt truss in Table 1 needs 28% more tonnage to achieve the same deflection as the Warren truss or 38% more material than the Bounded Optimal truss with 12 members.

The preceding examples certainly beg the question: How low can one go? The geometry of the lowest unbounded load path structure and the magnitude of its load path have been studied in the work of Mazurek and colleagues (2011; 2012) (see Figure 8). This research shows that the structure of minimal load path has a value of approximately $\sum F_T L_T + \sum F_C L_C = 13.17PB$. Once again, all the tension
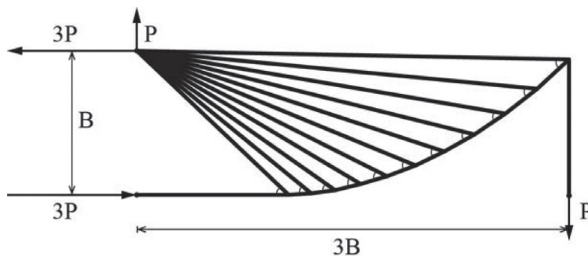
members intersect the compression members at the same angle. Although a structure in Figure 8 would generally be deemed impractical, it does provide a benchmark for judging alternate solutions. This will be discussed further in a later section.

AN APPLICATION OF MAXWELL'S THEOREM

For structures in which the external loads do not change as the geometry changes (generally simply supported structures), the dot product of the external forces and an arbitrarily selected origin will be a constant. Using this constant, Maxwell's theorem can determine the entire load path of a structure by calculating the constant and either the compression or tension load paths. The total load path is equal to twice the tension load path minus the constant or twice the compression load path plus the constant.

For example, consider Exchange House in London for which the first author (Baker) led the structural engineering team in the 1980s (Figure 9). This is a 10-story office building that spans over a series of rail lines and is supported by four 7-story parabolic arches. The author was not aware of Maxwell's load path theorem at the time of the design, so the geometry was developed using labor-intensive parametric studies. These parametric studies can be replaced by a simple application of Maxwell's theorem.

It can be inferred from Maxwell's theorem that if the tension load path is minimized, the total load path will also be minimized. To simplify calculations, the parameters B, H and W are used to describe the span and height of the building and the width tributary to an arch; z denotes the depth of the arch; and γ is the average density (weight including live load) of the building. In what follows, the columns and hangers will be simplified by considering them as a continuum.

The tension load path can be readily calculated, as shown in Figure 10. The force in the tie is equal to the overall moment in the system divided by the depth of the arch, $\gamma WHB^2/8z$; the length of the tie is equal to the width of the building, B. The total load path for the tie is $\gamma WHB^3/8z$. The load path of the hangers in Figure 10 can also be calculated as follows:
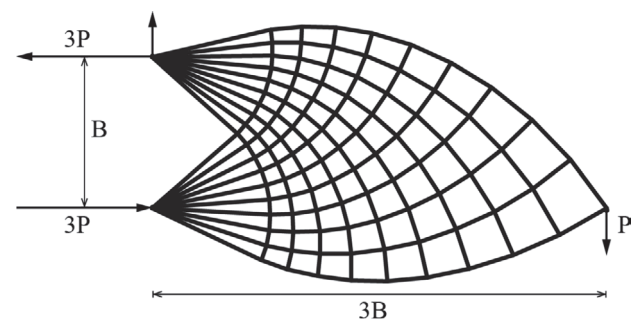

Fig. 8. *Optimal geometry for 3:1 cantilever based on the three-point load solution.*

Fig. 9. *Exchange House in London.*

$$\sum_{hangers} F_T L_T = 2 \int_0^{B/2} \int_0^{z\left(1-\left(\frac{2x}{B}\right)^2\right)} \gamma W y \; dy \; dx = \frac{4}{15} \gamma W B z^2 \quad (7)$$

Thus, the total tension load path is the sum of the tie and the hangers:

$$\sum F_T L_T = \sum_{hangers} F_T L_T + \sum_{tie} F_T L_T = \frac{4}{15}\gamma W B z^2 + \frac{\gamma W B^3 H}{8z}$$

$$(8)$$

The depth of the arch that will minimize the total load path of the structure (tension and compression load paths) can be found by taking a simple derivative of Equation 8:

$$\frac{d\left(\sum F_T L_T\right)}{dz} = 0 \Rightarrow \frac{8Bz}{15} - \frac{B^3 H}{8z^2} = 0 \Rightarrow z = \sqrt[3]{\frac{15B^2 H}{64}}$$

$$(9)$$

How does this result, based on a continuum, compare to the discrete problem with a finite number of columns and floors? Although not presented here, the authors have compared the results from Equations 8 and 9 to a calculation based on the discrete members of the Exchange House project and have found that the results are within 2%.

It should also be noted that the actual height of the Exchange House arch is lower than the optimum height because of a design requirement to find a close match of the parabolic arch to the grid of the columns and floors. The premium of the lower arch was deemed appropriate for the resulting simplicity of the connections, location of work-points, etc.

Maxwell's theorem can also be used to calculate the total load path of the structure. For this structure, the dot product, $\sum \vec{P_i} \cdot \vec{r_i}$, is a constant that is very easily calculated; it is equal to the load path that would exist if the building sat on the ground and was only supported by columns (Figure 11).

$$\sum \vec{P} \cdot \vec{r} = -\gamma B H W \cdot \frac{H}{2} \quad (10)$$

$$= -\frac{\gamma B H^2 W}{2}$$

Using twice the tension load path minus the constant, the total load path of the structure can be calculated as follows:

$$\sum_{total} FL = 2\left(\sum F_T L_T\right) - \sum \vec{P} \cdot \vec{r} \quad (11)$$

$$= 2\left(\frac{4}{15}\gamma W B z^2 + \frac{\gamma W B^3 H}{8z}\right) - \left(-\frac{\gamma W B H^2}{2}\right)$$

$$= \gamma B H W \left[\frac{8}{15}\frac{z^2}{H} + \frac{B^2}{4z} + \frac{H}{2}\right]$$

The total steel tonnage of the structure can now be estimated. For a structure of this scale, it is not unusual for the permitted tensile and compressive stresses for steel to be very similar. The tension members are controlled by the net-section issues; the compression members are controlled by buckling capacity. Dividing the total load path by an estimated average stress, σ, will provide an estimated total tonnage of steel.

Hopefully, this example helps the reader appreciate the power of Maxwell's theorem. The theorem enables the optimization for the conceptual design of a large structure and an estimate of the total tonnage of steel in a few short calculations without actually sizing a single member.

It is worth reflecting that the preceding process calculated the load path in the arch without directly calculating the forces in the arch. How is this possible? It is instructive to examine Figure 12. The load path in a diagonal member (such as a segment of an arch) is equal to the vertical component of the force times the vertical dimension of the member plus the horizontal component of the force times the horizontal dimension of the member. Using this knowledge, the following analysis shows how the arch load path is implicitly included.
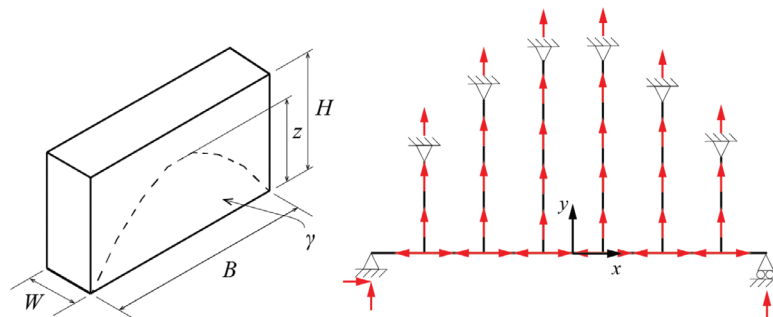

Fig. 10. Schematic of the building dimensions and tension members (tie and hangers) for Exchange House.

For the total structure (Figure 13), from Maxwell's theorem, it can be shown that

$$\sum_{total} FL = 2\sum_{tie} F_T L_T + 2\sum_{hangers} F_T L_T - \sum \vec{P} \cdot \vec{r} \qquad (12)$$

This must also be equal to

$$\sum_{total} FL = \sum_{tie} F_T L_T + \sum_{hangers} F_T L_T + \sum_{\substack{columns \\ above\ arch}} F_C L_C + \sum_{arch} F_C L_C \qquad (13)$$

The dot product in Equation 12 can be split into two values: the load path above the arch and the load path below the arch, as if the structure was supported directly on the ground:

$$\sum \vec{P} \cdot \vec{r} = -\sum_{\substack{columns \\ above\ arch}} F_C L_C - \sum_{\substack{columns \\ below\ arch}} F_C L_C \qquad (14)$$

Therefore, substituting into the total load path equation, the load path of the arch is simply

$$\sum_{arch} F_C L_C = \sum_{tie} F_T L_T + \sum_{hangers} F_T L_T + \sum_{\substack{columns \\ below\ arch}} F_C L_C \qquad (15)$$

which is shown graphically in Figure 14.

Here, we can see that the horizontal load path of the arch is equal to the horizontal load path of the adjacent tie plus the vertical load paths of the adjacent hangers plus the vertical load paths of the columns that were eliminated when the arch system was used instead of sitting directly on the ground. This is a remarkably sophisticated result from Maxwell's very simple equation.

MICHELL TRUSSES

In 1904, A.G.M. Michell wrote a seminal paper in which he outlined the principles of trusses with the shortest possible load paths and presented a limited number of solutions. Michell started with Maxwell's load path theorem and concluded that, if a continuous orthogonal deformation field is produced where all the tension elements are equally strained (elongated) and all the compression elements experience the same strain but are compressed, then the structure defined by these strain fields will be minimal, with the total load path of the structure equal to the work done by the external forces moving in this assumed displacement field. These displacement fields must satisfy certain mathematical relations and result in orthogonal tension and compression strain fields. It should be noted that the mathematics of these strain

Fig. 11. Schematic for Exchange House with column support only.
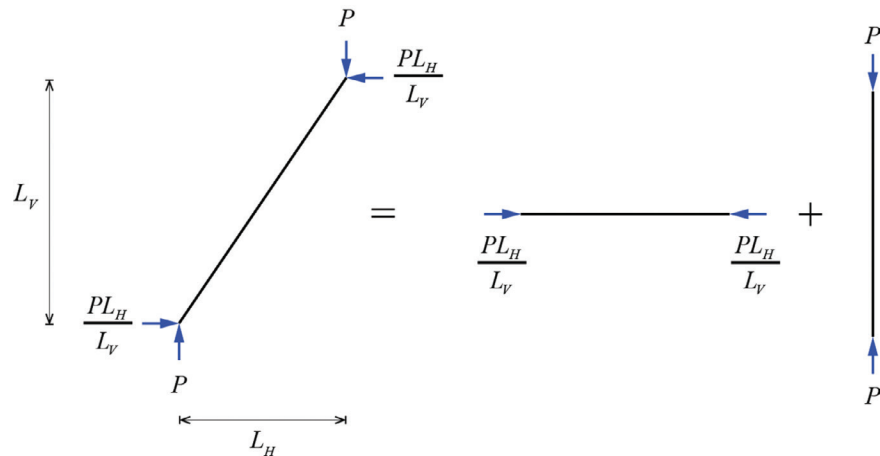
Fig. 12. Segment of an arch decomposed into a horizontal and vertical component.

fields are related to the slip lines in the Theory of Plasticity.

Discussed next are some of the truss geometries of minimal load path structures included in Michell's 1904 paper (see Figure 15). Because Michell approached the problem from the point-of-view of continuum mechanics, it should be noted that the following solutions permit an infinite number of elements (only a few of the members are drawn in the bicycle wheel like structures or the equilateral spirals of Figure 15). Nevertheless, Michell trusses are quite useful because they provide insight into optimal geometries and are benchmarks of the shortest possible load path for a

given structure. In the design of practical trusses, however, the final structures are composed of a finite number of elements. Thus, it is useful to look at the discretized versions of these optimal solutions, commonly referred to as discrete Michell trusses or discrete optimal trusses.

DISCRETE OPTIMAL TRUSSES

Research on discrete Michell trusses has produced results that are also useful in understanding optimal load path structures. Though these discrete Michell truss structures
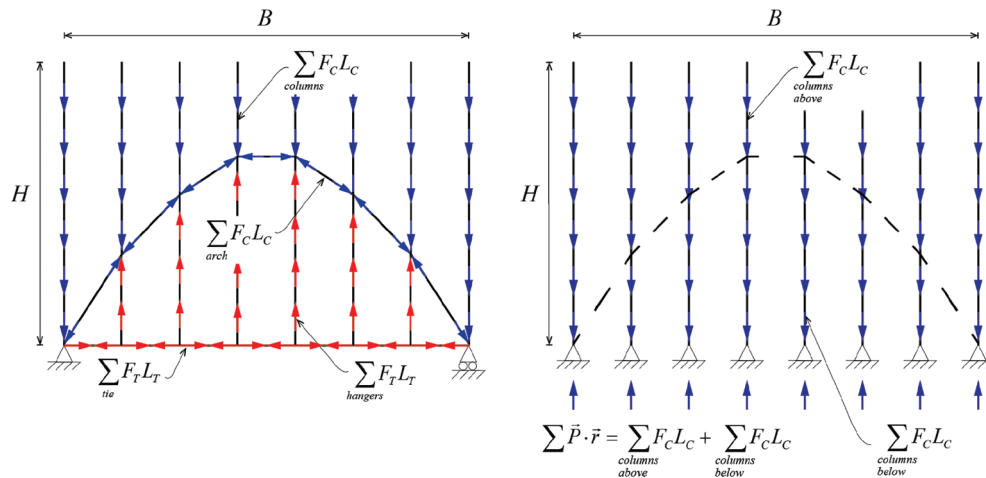

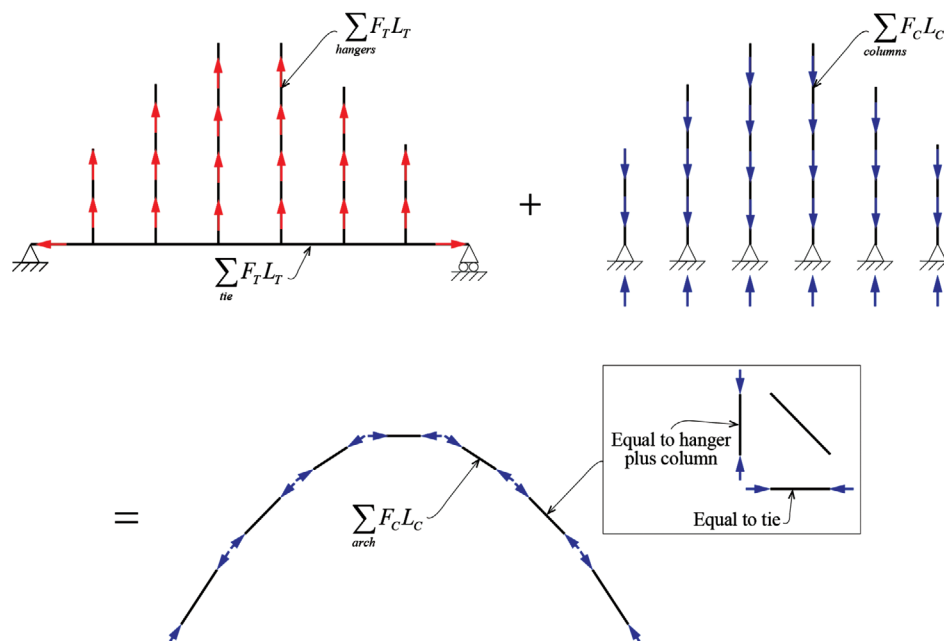Fig. 13.   Total load path of Exchange House.

Fig. 14.   Calculation of load path of the arch for Exchange House

are often impractical to build, they provide excellent benchmarks for designers in terms of efficiently utilizing materials. Recent work by Mazurek and colleagues (2011; 2012) and has shown that these discrete trusses can have amazing regularity and order. In the class of problems in which there is a symmetrical cantilever with two points of support and a single load, the complete geometry can be described using only one angle (denoted by α in Figure 16); the adjacent angles are right angles or complements of the first angle. An example can be seen in Figure 16, which was also studied by Chan (1960).

It is interesting to note that the optimal structure for the discrete Michell cantilever in Figure 16 is composed of several substructures, each of which is also optimal for the given number of members and connectivity. For example, the optimal geometry for a structure of two members is shown in the substructure, ξ_2, of Figure 16. Likewise, for eight members, the optimal structure is embedded in the larger optimal structures, composed of 18, 32, 50 and so on members. For a complete set of graphical rules to construct such geometries for three-point or three-force structures, the reader is referred to Mazurek and colleagues (2011; 2012).

The exact derivation of the optimal geometry for discrete trusses using Michell's theories or graphical rules, such as those shown by Mazurek and colleagues (2011), is often quite difficult for complicated loadings. Fortunately, today, designers have some powerful tools to assist in approximating optimal topologies for these more complex structures. Several of these tools include topology optimization using material distribution methods, such as the SIMP (Solid Isotropic Material with Penalization) material model (Bendsoe and Sigmund, 2002; Rozvany, Zhou and Birker, 1992), or discrete truss topology optimization methods based on ground structures (see Chapter 4 of Bendsoe and Sigmund, 2002, or Chapter 5 of Christensen and Klarbring, 2009). A brief overview of these tools is given in the following section.

TOPOLOGY OPTIMIZATION APPROACHES

According to Bendsoe and Sigmund (2002), topology optimization consists of studying the optimal arrangement of isotropic material in space for the design of the topology of a structure. A geometric representation of such a structure can be thought of as a black-and-white rendering of an image, in which the "pixels" are given by finite elements. This methodology essentially starts with a uniformly distributed "gray" material in which the optimal layout is determined through an iterative process to reveal a potentially optimal load path, represented by "black" and "white" densities. An example of this methodology can be seen in Figure 17 using the educational codes provided in Talischi and colleagues (2012a; 2012b) for the topology optimization of a 6:1 simple span problem with five sets of uniformly spaced point loads. One of the major advantages of this methodology is that the feasible solutions can have any size, shape or connectivity. For an example of the use of topology optimization in the design of steel bracing systems of high-rise buildings, refer to Stromberg and colleagues (2012).

An alternative approach based on ground structures considers a form of gridlike continua for the topology optimization of trusses using discrete members; this can also be viewed as a sizing problem where the connectivity must be specified *a priori*. Within these techniques, there are literally thousands of interconnected truss elements that coalesce into patterns based on the final optimal cross-sectional areas that reveal optimal (minimal) load path structures. To generate such topologies using this approach, refer to the educational code provided in Sokol (2011); see Figure 18.

The interpretation of the results computed using either of these tools requires a significant amount of engineering judgment and an understanding of practical issues such as constructability and functionality of the truss. Using these solutions, a discrete truss, which provides the general connectivity of the structure, can be interpreted. However, the
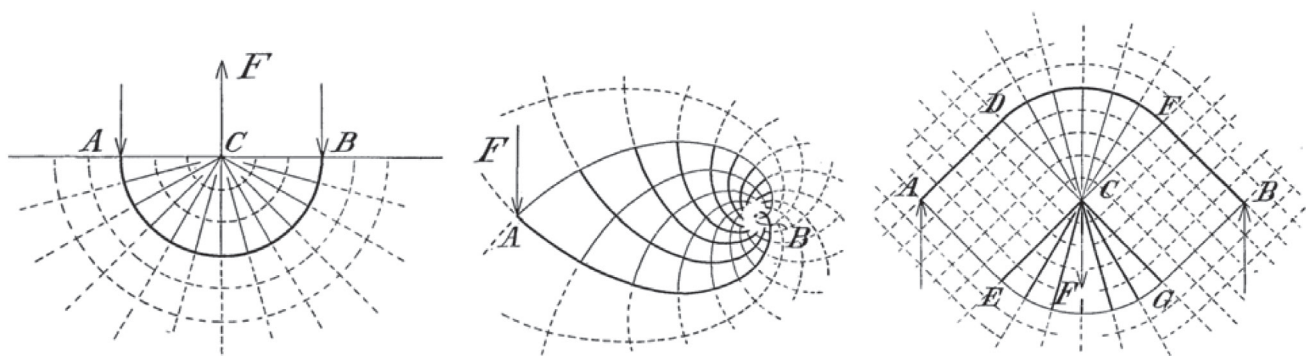

Fig. 15. Minimal load path structures taken from Michell (1904): semi-infinite fan (left),
orthogonal systems of equiangular spirals (center) and centrally loaded beam (right).

determination of the precise location of the joints (nodes) can be quite subjective because it is often an "eyeball" estimate of the location. Therefore, after the connectivity is identified, the final "optimal" locations of the nodes might then be refined using various searching or gradient optimization techniques. One useful method that also gives great insight into the forces in the individual members is Graphic Statics.

GRAPHIC STATICS

Graphic Statics is a powerful tool for studying both the geometry and the forces in a structure using only graphical methods. It was once in wide usage, initially based on the work of Rankine and Maxwell and later adopted and refined by Culmann and Cremona. Graphic Statics has recently been revived in the design of compression-only masonry shells in the work of Block and Ochsendorf (2007).

Graphic Statics uses graphical techniques to determine the axial forces in certain common trusses geometries. It was originally done with simple drafting tools and can now be easily done with computer graphic programs or simple spreadsheets. It does not require the calculation of stiffness,
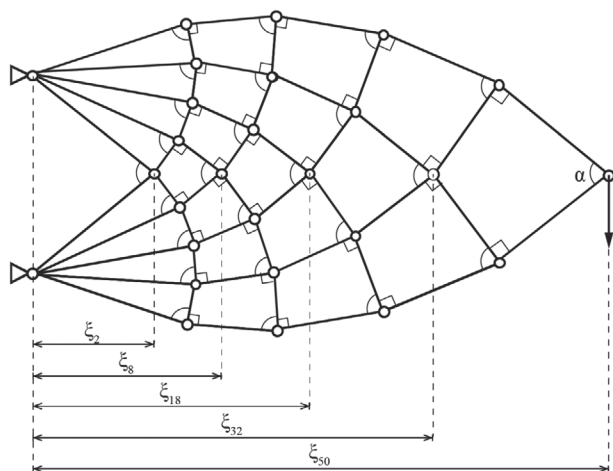
only simple geometrical relationships. It produces two diagrams—one that represents the geometry of the truss and the other that represents the axial forces in the members of the truss. Maxwell determined that these two diagrams are reciprocal.

Cremona later modified this concept so that, for each line in the form diagram (truss geometry), there is a parallel line in the force diagram, the length of which is proportional to axial force in the original form line (truss member). Maxwell also determined that each node in the form diagram maps into a closed polygon in the force diagram, which represents the equilibrium of the forces at the node. Also, every polygon in the form diagram maps into a node in the force diagram. Because these two diagrams are reciprocal, the mapping can also be reversed. This means that the designer can manipulate the force diagram in order to determine the geometry that produces a desired set of forces.

As described by Baker and colleagues (2013), for a given connectivity of nodes, Graphic Statics provides all the information needed to determine the total load path of the structure in the form and force diagrams; that is, using the form diagram, the member lengths can be found while the force diagram provides the corresponding member forces. Thus, all of the information is graphically available to determine the total load path.

To understand the mappings between the reciprocal diagrams, consider the simple six-panel gable truss (Zalewski and Allen, 1998) shown in Figure 19. On the left, the geometry of the structure, or the form diagram, is shown. The lines in the form diagram represent structural members or, rather, lines of action of the structural members. The lines in the second diagram (on the right of Figure 19), known as the force diagram, represent forces carried by the members from the form diagram. In this figure, dashed line vectors are used to represent these external forces both in the form and force diagrams.

The notation used in Figure 19 and following diagrams is an interval notation based on a version of Bow's notation (Bow, 1873). For the form diagram, the capital letters, *A*, *B*, *C*, … , are sequentially placed clockwise in the intervals between external forces (open polygons) and numbers, 1, 2, 3, … , are placed in the internal spaces (closed polygons)

Fig. 16. *Optimal discrete Michell truss.*

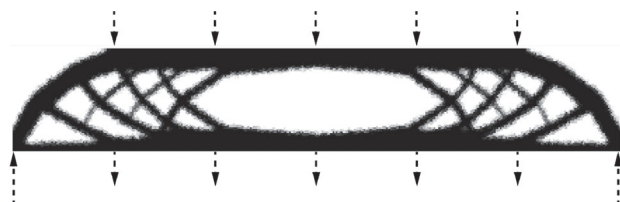Fig. 17. *Topology optimization approach by distribution of isotropic material using the educational code, PolyTop (Talischi et al., 2012a; 2012b).*
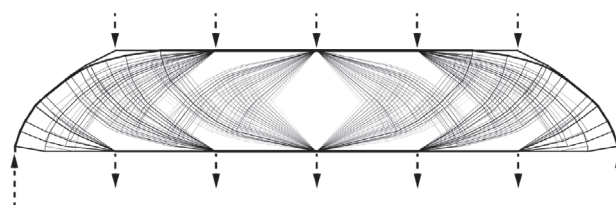

Fig. 18. *Topology optimization approach using ground structures, computed by the educational code in Sokol (2011).*

between members. Each line in the form diagram is bordered by two polygons. Thus, a member may be referred to using the corresponding letter or number of the adjacent polygons—for example, A-1 or 2-3—and a joint called with a series of letters and numbers—for example, A-B-3-2-1-A. Similarly, the external forces are referenced using the adjacent open polygons—for example, F_{AB}. The open polygons denoted by capital letters in the form diagram correspond to points (nodes) on the load line of the force diagram, denoted by the lowercase letters, $a, b, c, \ldots$. The numbers denoting the closed polygons in the form diagram also have corresponding nodes in the force diagram.

This graphical methodology allows the user to determine the axial force in a truss member by measuring the length of the reciprocal line in the force diagram. The relative magnitude of the force diagram is set by drawing the load line, which represents the external forces, to scale. For example, the force in member A-1 in the form diagram of Figure 18 is proportional to the length of the line between points a and 1 in the corresponding force diagram. Similarly, the force in the member between polygons 2 and 3 is proportional to the length of the line between points 2 and 3 of the force diagram. The remaining forces in the other members can be computed likewise. It should be noted that nodes 1 and 2 overlay each other in the force diagram; this indicates that member 1-2 has zero force (the same is true for member 9-10). Thus, the forces acting on a node in the form diagram correspond to a polygon in the force diagram, where each force is a side of the polygon. For example, at node A-B-3-2-1-A, the polygon of forces is given by points a-b-3-2-1-a. Reading clockwise around joint A-B-3-2-1-A in the form diagram, we can determine if members A-1 and 2-3 are in tension or compression. If read from 1 to a on polygon a-b-3-2-1-a, we move from the lower left to the upper right, toward the joint A-B-3-2-1-A of the form diagram. Thus, member A-1 is in compression. Likewise, moving from 3 to 2 on the force polygon goes from the lower right to the upper left, or

toward the joint in the form diagram, so member 3-2 is also in compression. For more details on reciprocal relationships, refer to Baker and colleagues (2013) and Zalewski and Allen (1998).

A useful application of Graphic Statics for structural design has also been described in Chapter 14 of the book by Zalewski and Allen (1998) for form-finding of trusses by graphically solving for the nodal locations that give a constant chord-force truss. For example, the gable truss of Figure 19 is revisited in Figure 20, in which the objective becomes to find the geometry of a truss in which the force in the top chord is constant. This can be accomplished by manipulating the force diagram so that the lengths of lines a-1, b-3, c-5, d-6, e-8 and f-10 are the same, representing equal forces. After the force diagram is modified to achieve the desired properties, work backward to find the reciprocal form diagram, resulting in the desired geometry. This has been applied in the design of the structure by Robert Maillart shown in Figure 21. Note that the forces in members 2-3, 4-5, 6-7 and 8-9 are zero because the nodes are overlaid in the force diagram on the right. These members were eliminated from Maillart's structure.

Similarly, to find the geometry of the truss in which there is a constant force in both the top and bottom chords, the force diagram can be modified accordingly so that all lines in the force diagram corresponding to the members in the chords have the same length. This example can be seen in Figure 22.

The authors note that the force polygon and form diagrams can be manipulated in this figure to achieve higher or lower forces and shallower or deeper trusses, depending on the needs of the designer. Also, members 2-3, 4-5, 6-7 and 8-9 are all zero force members. They may still be required for considerations of stability or unbalanced loads, unless the chords have sufficient flexural strength and stiffness to address these issues.

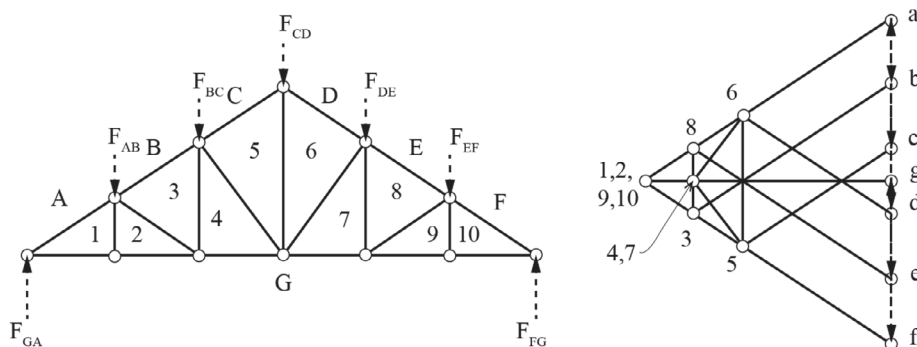As previously mentioned, an interpretation of topology

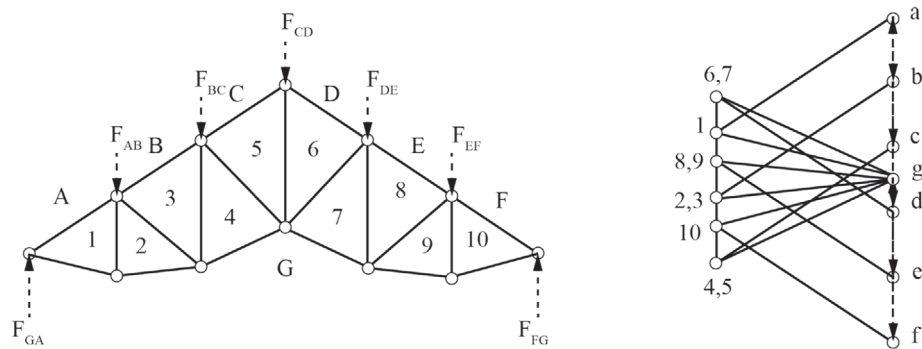Fig. 19. Form and force diagrams for gable truss.

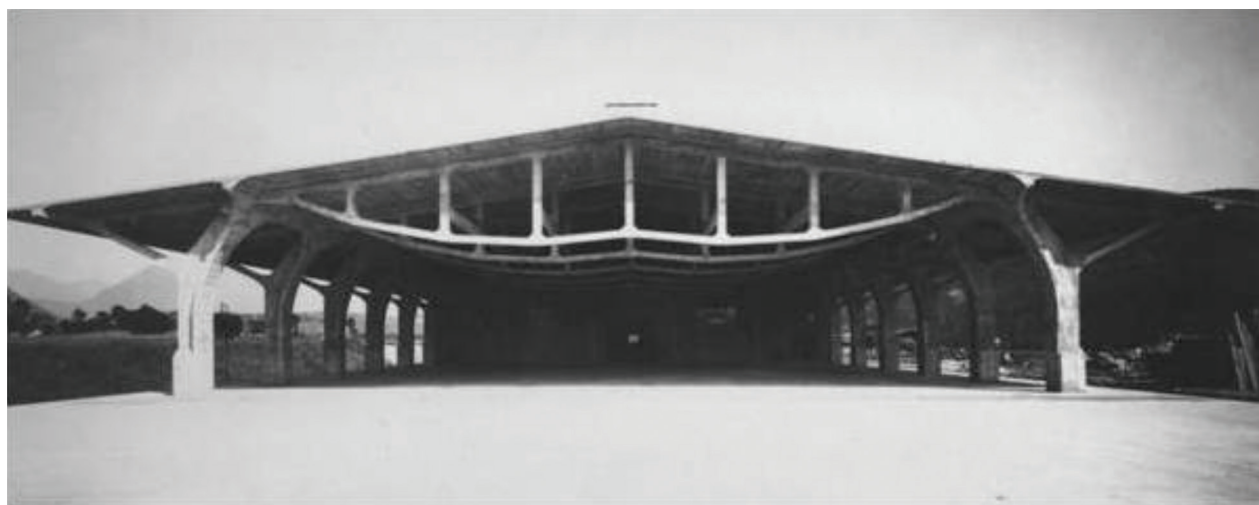*Fig. 20. Constant force gable truss (force is constant in top chord).*

Fig. 21. Design using form-finding of a constant-force gable truss (Zalewski and Allen, 1998).
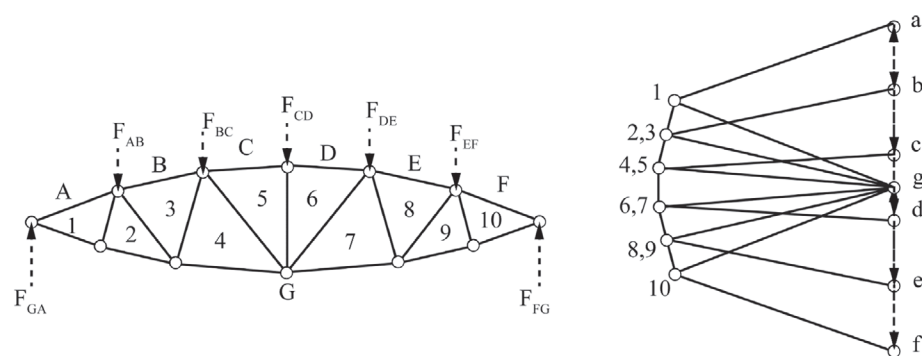

Fig. 22. Truss designed for constant and equal force in top and bottom chord.

optimization solutions from continuum or ground structure approaches provides approximate nodal locations and connectivity. Refinement of the nodal locations can be achieved through manipulation of the force diagram in graphic statics.

Figures 17 and 18 show the results of a continuum topology optimization by means of material distribution and ground structures, respectively. These results were then interpreted into general truss configurations, which give the general connectivity of nodes. To find a more precise location of nodes, various optimization techniques can be used. One method is to manipulate the force diagram of a graphic statics analysis until a minimum total load path is achieved. The reason the force diagram is manipulated rather than the form diagram is because we can always be assured that the solution is in equilibrium because the force polygons will always close. It can also be noted that because the solution is automatically constrained to be in equilibrium, there are fewer independent variables than if we tried to manipulate the form diagram. The result of this exercise is shown as truss A in Table 2. These solutions provide benchmarks against which the other truss geometries in Table 2 can be compared. It is worth noting that the geometry has a substantial influence on the potential efficiency of a truss, particularly when the design is deflection controlled. The geometry of the discrete optimal truss (truss A) is not common but is extremely regular, with the tension members intersecting the compression members at consistent angles.

The structural volume comparisons in Table 2 are appropriate for situations in which the permissible tensile and compressive stresses are similar in magnitude. The Warren truss, the combined Warren/Pratt truss and the compression diagonal Pratt truss (trusses C, D and E, respectively) have relatively short load paths and are appropriate for heavy trusses with stocky web members. They also have the advantage of having compression connections for the web members with the largest forces. Compression connections are often more efficient than tension connections for large forces.

The ranking of the truss geometries would change if the permitted compressive stresses were sensitive to the unbraced lengths. Trusses A and B would still have relatively low volumes because of the reduced unbraced lengths of the web members. To take full advantage of these geometries, designers need to consider the stabilizing effects of the tension diagonals and the benefits of connection continuity when determining the capacity of the compression diagonals in trusses A and B. These effects greatly increase the in-plane and out-of-plane buckling strength of the compression diagonals; the AISC direct analysis method is a good approach for capturing this benefit. Using this method, the effective length factor K can be set equal to 1.0 for all the members, and by considering a second-order numerical analysis with modified members' stiffness, it is possible to capture the increased strength in the members.

The Pratt truss with tension diagonals (truss F) is often an appropriate geometry for trusses with slender members where the permitted compressive stresses are very sensitive to unbraced length. In such situations, truss F may have less tonnage than the trusses with compression diagonals. Truss F also benefits from fewer connections than trusses A and B and may be easier to erect than trusses with compression diagonal at the support. When considering a geometry similar to truss F, the designer should understand that the truss has a fundamentally longer total load path; some of the savings in web members will be offset with additional forces in chords and web members, as well as increased deflections. These "hidden" penalties are often overlooked when the designer only studies the web members when determining the geometry of a truss.
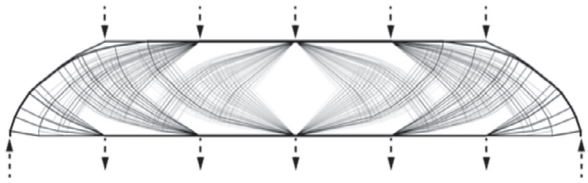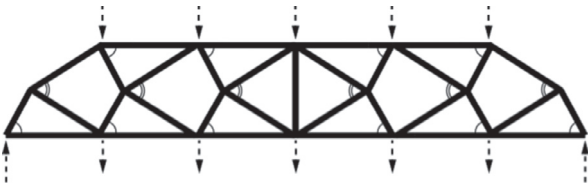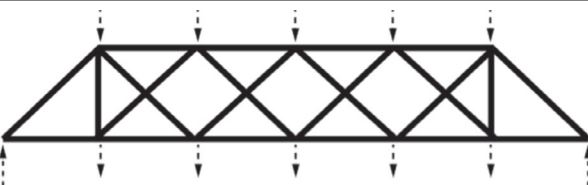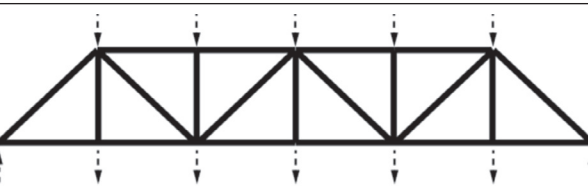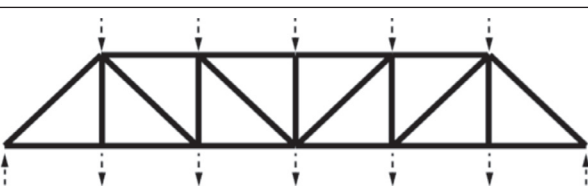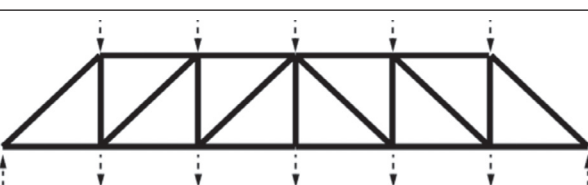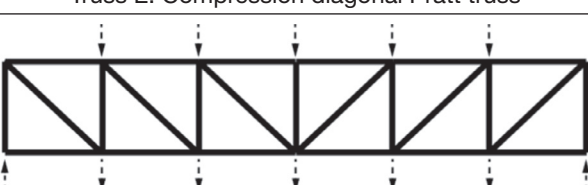
CONCLUSIONS

Several years ago, the first author (Baker) heard a reference to Michell trusses while attending an overseas conference. An attempt to learn more about the subject prompted the purchase of an out-of-print book that included Michell's 1904 paper. The work was both illuminating and thought-provoking. Exploration of Michell's work led the authors to Maxwell. Unfortunately, while Maxwell produced an immense body of work, much of it is unrelated to structural engineering. Seeking a guide to Maxwell, the authors turned to the *History of Strength of Materials* by Timoshenko (1953). This inquiry into Maxwell ultimately led the authors to Rankine, Cremona and a reexamination of Airy. Amazingly, several of their important ideas are no longer common currency (or may have never been widely known). The search for lost ideas continues.

Maxwell's load path theorem is simple and powerful. Inefficiencies must be paid for twice—once in tension and once in compression. Minimize one and the other is also minimized. Michell trusses provide benchmarks for least load path solutions. Discrete Michell trusses are amazingly regular and ordered; their shapes both surprising and informative. While Graphic Statics has been replaced by the computer as an analysis tool, it remains a powerful design tool. Modern topology optimization tools make finding efficient layouts for complex problems accessible to the designer. The authors have found that these ideas and tools greatly aid in the conceptual design of trusses and other structures.

The working title for this paper was "things I wish I had

Table 2. Relative Efficiency of Various Trusses Compared to Minimum Load Path Structures			
Discretized Solution	**Volume Ratio for Constant Stress**	**Deflection for Constant Stress**	**Volume Ratio for Equal Deflection**
Ground structures solution	100%	100%	100%
Truss A: Discretized optimal truss	102.6%	102.6%	105.3%
Truss B: Lattice truss	111.6%	111.6%	124.7%
Truss C: Warren truss	111.6%	111.6%	124.7%
Truss D: Combined Warren/Pratt truss	113.7%	113.7%	129.2%
Truss E: Compression diagonal Pratt truss	119.7%	119.7%	143.3%
Truss F: Tension diagonal Pratt truss	129.8%	129.8%	168.4%

known when I started designing structures." None of the preceding theorems, tools or techniques was included in the authors' engineering education, but all are useful in developing an efficient structural design. Quite simply, the potential efficiencies or inefficiencies of a design are determined by the structural geometry. No amount of optimizing the size of individual members will compensate for a bad structural layout. The authors hope that the paper makes this information available to today's structural engineering educators and practicing structural engineers so that they can create efficient designs that conserve our resources and reduce the carbon footprint of our construction.

REFERENCES*

Airy, G.B. (1863), "On the Strains in the Interior of Beams," *Philosophical Transactions of the Royal Society of London*, Vol. 153, pp. 49–71.

Baker, W.F., Beghini, L.L., Mazurek, A., Carrion, J. and Beghini, A. (2013), "Maxwell's Reciprocal Diagrams and Discrete Michell Frames," *Structural and Multidisciplinary Optimization*, Vol. 48, Issue 2, pp. 267–277.

Beghini, A., Beghini, L.L., Schultz, J.A., Carrion, J. and Baker, W.F. (2013), "Rankine's Theorem for the Design of Cable Structures," *Structural and Multidisciplinary Optimization*, Vol. 48, Issue 5, pp. 877–892.

Bendsoe, M.P. and Sigmund, O. (2002), *Topology Optimization: Theory, Methods and Applications*, Springer, Berlin.

Block, P. and Ochsendorf, J. (2007), "Thrust Network Analysis: A New Methodology for Three-Dimensional Equilibrium," *Journal of the International Association for Shell and Spatial Structures*, Vol. 48, No. 3, pp. 1–8.

Bow, R.H. (1873), *Economics of Construction in Relation to Framed Structures*, ICE Publishing, London.

Chan, A.S.L. (1960), "The Design of Michell Optimum Structures," Ministry of Aviation Aeronautical Research Council Report, No. 3303, pp. 1–40.

Christensen, P.W. and Klarbring, A. (2009), *An Introduction to Structural Optimization*. Springer.

Cox, H.L. (1965), *The Design of Structures of Least Weight*, Pergamon Press, Oxford, United Kingdom.

Forfar, D.O. (2012), "Maxwell, Einstein, Newton and Faraday," *Newsletter of the James Clerk Maxwell Foundation,* Vol. 1, p. 2.

Maxwell, J.C. (1864), "On Reciprocal Figures and Diagrams of Forces," *Philosophical Magazine*, Vol. 26, pp. 250–261.

Maxwell, J.C. (1870), "On Reciprocal Figures, Frames, and Diagrams of Forces," *Edinbrook Royal Society Proceedings*, Vol. 7, pp. 160–208.

Mazurek A. (2012). "Geometrical Aspects of Optimum Truss-Like Structures for Three-Force Problem," *Structural and Multidisciplinary Optimization*, Vol. 45, No. 1, pp. 21–32.

Mazurek, A., Baker, W.F. and Tort, C. (2011), "Geometrical Aspects of Optimum Truss-Like Structures," *Structural and Multidisciplinary Optimization*, Vol. 43, No. 2, pp. 231–242.

Michell, A.G.M. (1904), "The Limits of Economy of Material in Frame-Structures," *Philosophical Magazine*, Vol. 8, No. 47, pp. 589–597.

Rozvany, G.I.N., Zhou, M. and Birker, T. (1992), "Generalized Shape Optimization without Homogenization," *Structural and Multidisciplinary Optimization,* Vol. 4, No. 3, pp. 250–252.

Sokol, T. (2011), "A 99 Line Code for Discretized Michell Truss Optimization Written in Mathematica," *Structural and Multidisciplinary Optimization*, Vol. 43, pp. 181–190.

Stromberg, L.L., Beghini, A., Baker, W.F. and Paulino, G.H. (2012), "Topology Optimization for Braced Frames: Combining Continuum and Beam/Column Elements," *Engineering Structures*, Vol. 37, pp. 106–124.

Talischi, C., Paulino, G.H., Pereira, A., and Menezes, I.M.F. (2012a), "PolyMesher: A General-Purpose Mesh Generator for Polygonal Elements Written in Matlab," *Structural and Multidisciplinary Optimization*, Vol. 45, No. 3, pp. 309–328.

Talischi, C., Paulino, G.H., Pereira, A., and Menezes, I.M.F. (2012b), "PolyTop: A Matlab Implementation of a General Topology Optimization Framework Using Unstructured Polygonal Finite Element Meshes," *Structural and Multidisciplinary Optimization*, Vol. 45, No. 3, pp. 329–357.

Timoshenko, S.P. (1953), *History of Strength of Materials*. McGraw-Hill Book Company, New York.

Zalewski, W. and Allen, E. (1998), *Shaping Structures: Statics*. John Wiley & Sons, New York.

---

* Many of the older references are within the public domain and can be downloaded from Google Books.